Simple potential-flow model of Rayleigh-Taylor and Richtmyer-Meshkov instabilities for all density ratios

Sung-Ik Sohn*
Division of Science, Tongmyong University of Information Technology, 535 Yongdang-dong, Pusan 608-711, Korea
(Received 4 July 2002; published 5 February 2003)

We generalize the Layzer-type model for unstable interfaces to the system of arbitrary density ratio. The predictions from the generalized model for bubble growth rates of Rayleigh-Taylor (RT) and Richtmyer-Meshkov (RM) instabilities are in good agreement with numerical results. We present the theoretical prediction for asymptotic growth rates for RT and RM bubbles for finite density ratios in two and three dimensions.

DOI: 10.1103/PhysRevE.67.026301 PACS number(s): 47.20.Ma, 47.20.Ky

The phenomenon of unstable interfacial fluid mixing occurs frequently in basic sciences and engineering applications. A gravity-driven interfacial instability is known as the Rayleigh-Taylor (RT) instability [1] and a shock-driven interfacial instability is known as the Richtmyer-Meshkov (RM) instability [2]. Both instabilities play important roles in many fields such as inertial confinement fusion and supernova. To investigate dynamics of these instabilities, extensive researches have been carried out in last decades. Recent progress on the study of RT and RM instabilities can be found and traced from Refs. [3–13].

The linear stage of small perturbation amplitude $k\eta \ll 1$, where k is the perturbation wave number, is well understood [1,2]. As the amplitude becomes large $k\eta \sim 1$, the nonlinear structure in the form of bubbles and spikes appears on the unstable interfaces. A bubble (spike) is a portion of the light (heavy) fluid penetrating into the heavy (light) fluid. At later times, a bubble in the RT instability attains a constant velocity, while a RM bubble has a decaying growth rate. Eventually, a turbulent mixing caused by vortex structures around spikes breaks the ordered fluid motion [3,8].

Weakly nonlinear theories [5,6] based on higher-order series expansions of equations give growth rates for interfaces up to early nonlinear regime, but fail to provide growth rates at late times. Layzer [14] proposed a potential flow model, based on the approximate description of the flow near the bubble tip, and successfully described the evolution of a single-mode RT bubble over all times. Since Layzer's work, the model was extended to a bubble for the RM instability by Hecht *et al.* and to spikes for RT and RM instabilities by Zhang [9]. However, most of the previous Layzer-type models have been limited to the system with an infinite density ratio.

In this paper, we generalize the Layzer-type model to the unstable system for arbitrary density ratio. The predictions from our approach are in good agreement with numerical results for both RT and RM instabilities over all times. Our approach also provides analytic solutions for asymptotic growth rates of single-mode RT and RM bubbles in the system of finite density ratio in two and three dimensions.

Note that the asymptotic solution of single-mode bubbles at unstable interfaces not only has its own fundamental importance, but also is a key factor in the dynamics of the bubble merger in the evolution of multimode interfaces [3,8].

We consider an interface in a channel of width L filled with two fluids of different densities in two dimensions (See Fig. 1). The fluids are assumed as incompressible and inviscid. We denote densities of upper and lower fluids as ρ and ρ', respectively. As shown in Fig. 1, the bubble pushes the upper fluid and has a rounded shape, while the spike penetrates the lower fluid and has a mushroom shape due to vorticities by the Kelvin-Helmholtz instability. Note that, for the case of infinite density ratio, the spike is a form of long and narrow filament without the vortex structure.

The flow around the bubble can be assumed as irrotational, since the bubble has a smooth laminar structure. From the assumption of potential flows, each fluid around the bubble is governed by

$$\Delta\phi(x,z,t)=0 \quad \text{for upper fluid,} \tag{1}$$

$$\Delta\phi'(x,z,t)=0 \quad \text{for lower fluid.} \tag{2}$$

where ϕ, ϕ' are velocity potentials. The evolution of the interface, $z=\eta(x,t)$, can be determined by the kinematic equation

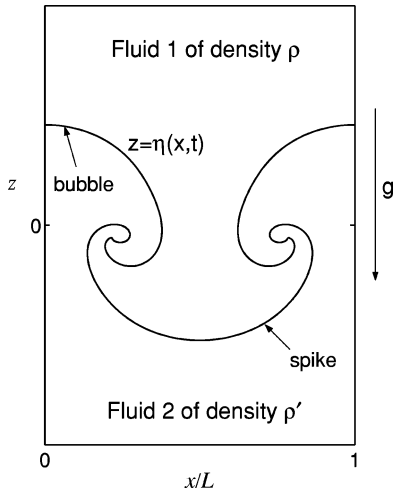

FIG. 1. Flow description. g represents an external acceleration.

*Electronic address: sohnsi@tmic.tit.ac.kr

$$\frac{\partial \eta}{\partial t} + u\frac{\partial \eta}{\partial x} - v = 0, \tag{3}$$

and the Bernoulli equation

$$\rho\frac{\partial \phi}{\partial t} + \frac{\rho}{2}\left[\left(\frac{\partial \phi}{\partial x}\right)^2 + \left(\frac{\partial \phi}{\partial z}\right)^2\right] + \rho g z = \rho'\frac{\partial \phi'}{\partial t} + \frac{\rho'}{2}\left[\left(\frac{\partial \phi'}{\partial x}\right)^2 + \left(\frac{\partial \phi'}{\partial z}\right)^2\right] + \rho' g z. \tag{4}$$

Here, u and v are x and z components of the interface velocity, respectively, and g is an external acceleration.

Extending Layzer's, we take velocity potentials

$$\phi(x,z,t) = a(t)\cos(kx)e^{-kz}, \tag{5}$$

$$\phi'(x,z,t) = -a(t)\cos(kx)e^{-kz}. \tag{6}$$

where the wave number $k = 2\pi/L$. The velocity fields for each fluid are defined as

$$\mathbf{q} = \nabla\phi \quad \text{for upper fluid,} \tag{7}$$

$$\mathbf{q} = -\nabla\phi' \quad \text{for lower fluid.} \tag{8}$$

The corresponding stream functions for Eqs. (5) and (6) are $\psi(x,z,t) = a(t)\sin(kx)e^{-kz}$ and $\psi'(x,z,t) = -a(t)\sin(kx)e^{-kz}$. The streamlines generated by $\psi(x,z,t) = \psi(x_0,z_0,t)$ and $\psi'(x,z,t) = \psi'(x_0,z_0,t)$, passing through an arbitrary reference point (x_0,z_0), are

$$z = z_0 + \frac{1}{k}\ln\left(\frac{\sin kx}{\sin kx_0}\right). \tag{9}$$

The interface velocity, $\mathbf{U} = (u,v)$, is defined as the average of velocities below and above the interface

$$\mathbf{U} = \frac{1}{2}(\nabla\phi - \nabla\phi') \quad \text{at } z = \eta. \tag{10}$$

The shape of the interface near a bubble tip is, under the parabola approximation,

$$\eta(x,t) = h(t) + \xi(t)x^2. \tag{11}$$

Then, from Eqs. (10) and (11), components of the interface velocity are $u \sim -ak^2e^{-kh}x$ and $v \sim -ake^{-kh}[1-(k^2/2 + k\xi)x^2]$. Substituting these expressions into Eqs. (3) and (4) and expanding it up to the second order in x, we have the following equations:

$$\frac{dh}{dt} = -ake^{-kh}, \tag{12}$$

$$\frac{d\xi}{dt} = ak^2\left(3\xi + \frac{k}{2}\right)e^{-kh}, \tag{13}$$

$$ke^{-kh}\left(\xi + \frac{k}{2}\right)\frac{da}{dt} + Aa^2k^3\xi e^{-2kh} - Ag\xi = 0, \tag{14}$$

where $A = (\rho-\rho')/(\rho+\rho')$ represents the Atwood number. The differential equations (12)–(14) determine the evolutions of bubbles in RT and RM instabilities.

It has been shown in Refs. [7,14] that the linear theory of Layzer's model for infinite density ratio agrees with the result from the linearized Euler equations. One can easily show that this property also holds for the present model for finite density ratios.

We now find asymptotic solutions for bubbles. Eliminating a from Eqs. (12) and (13), we have

$$\xi(t) = \left(\xi_0 + \frac{k}{6}\right)e^{-3k(h-h_0)} - \frac{k}{6}, \tag{15}$$

where $\xi_0 = \xi(t=0)$ and $h_0 = h(t=0)$.

We introduce a new variable

$$H(t) = e^{kh(t)}. \tag{16}$$

Then, Eq. (14) is written in the form

$$-\left(1 + \frac{k}{2\xi}\right)H\frac{d^2H}{dt^2} + A\left(\frac{dH}{dt}\right)^2 - AkgH^2 = 0. \tag{17}$$

To derive asymptotic solutions for bubbles, we consider behaviors for large $h(t)$. For $kh(t) \gg 1$, $\xi \to -k/6$ by Eq. (15), so that Eq. (17) becomes, approximately,

$$2H\frac{d^2H}{dt^2} + A\left(\frac{dH}{dt}\right)^2 - AkgH^2 = 0. \tag{18}$$

For the RT instability ($g = \text{const} > 0$), Eq. (18) has the solution

$$H(t) = e^{\alpha t}, \tag{19}$$

with $\alpha = \sqrt{Akg/(A+2)}$. This leads to the asymptotic solution

$$\nu_{\mathrm{RT}}^{\infty} \to \sqrt{\frac{Ag}{(2+A)k}}, \quad \xi_{\mathrm{RT}}^{\infty} \to -\frac{k}{6}. \tag{20}$$

Here, ν denotes dh/dt and the superscript ∞ represents a quantity at asymptotic large time. For the RM instability ($g = 0$), Eq. (18) has the solution

$$H(t) = t^{\beta}, \tag{21}$$

with $\beta = 2/(A+2)$. Thus, the asymptotic solution is

$$\nu_{\mathrm{RM}}^{\infty} \sim \frac{2}{(2+A)kt}, \quad \xi_{\mathrm{RM}}^{\infty} \to -\frac{k}{6}. \tag{22}$$

Therefore, the growth rate of a RT bubble in the system of finite density ratios converges to an asymptotic limit and that of a RM bubble decays to zero. For both RT and RM insta-

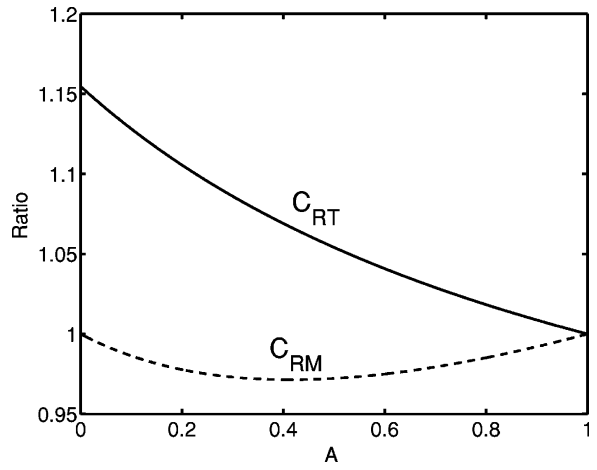

FIG. 2. Ratios of solutions for asymptotic bubble velocities. $C_{\mathrm{RT}}=\sqrt{2/3(1+A)}/(1/\sqrt{2+A})$ for the RT case, and $C_{\mathrm{RM}}=[(3+A/3(1+A)]/[2/(2+A)]$ for the RM case.

bilities, the asymptotic velocities of bubbles are independent of initial conditions. We see that, fixing g and k, the asymptotic velocity for a RT bubble is an increasing function of the Atwood number A, while that for a RM bubble is a decreasing function of A.

Recently, Goncharov [13] has extended the Layzer model to the system of arbitrary density ratio, using different forms of velocity potentials from ours. Since the Layzer model is an approximate description for the flow around the bubble tip, various forms of approximate potentials can be given to the system. The potentials (5) and (6) used in our approach may be the simplest ones among possible approximate potentials for the case of arbitrary density ratio. In Goncharov's study, the velocity potential for the lower fluid has two unknowns, which results in five sets of differential equations. The asymptotic bubble velocities for two dimensions (2D) given in Ref. [13] are

$$\nu_{\mathrm{RT}}^{\infty}\rightarrow\sqrt{\frac{2Ag}{3(1+A)k}},\quad \xi_{\mathrm{RT}}^{\infty}\rightarrow-\frac{k}{6}, \tag{23}$$

and

$$\nu_{\mathrm{RM}}^{\infty}\sim\frac{(3+A)}{3(1+A)kt},\quad \xi_{\mathrm{RM}}^{\infty}\rightarrow-\frac{k}{6}. \tag{24}$$

The functional expressions of Eqs. (20) and (22) for asymptotic velocities are different from Eqs. (23) and (24). However, quantitative differences between these solutions are not large. Figure 2 shows ratios of Eqs. (20) and (23), $C_{\mathrm{RT}}=\sqrt{2/3(1+A)}/(1/\sqrt{2+A})$ for the RT case, and ratios of Eq. (22) and (24), $C_{\mathrm{RM}}=[(3+A)/3(1+A)]/(2/(2+A)]$ for the RM case. We see that the difference of asymptotic solutions for the RT case is small for large A and slightly large for small A, while that for the RM case is small for all A.

For limiting values of A, analytic solutions for finite times can be derived. Differentiating Eq. (12) and substituting it into Eq. (14), we have

$$\frac{d^2h}{dt^2}+\frac{2(1-A)k\xi+k^2}{2\xi+k}\left(\frac{dh}{dt}\right)^2+\frac{2Ag\xi}{2\xi+k}=0. \tag{25}$$

From the relation $d^2h/dt^2=(d\xi/dt)(d\nu/d\xi)=-(k/4)(6\xi+k)(d\nu^2/d\xi)$, Eq. (25) becomes

$$\frac{d\nu^2}{d\xi}-\frac{4(2(1-A)\xi+k)}{(6\xi+k)(2\xi+k)}\nu^2-\frac{8Ag\xi}{k(6\xi+k)(2\xi+k)}=0. \tag{26}$$

Then, the solution for the case of $A\rightarrow 0$ is

$$\nu=Q^r\left[\frac{Ag}{2k}(G-G_0)+\frac{\nu_0^2}{Q_0^{2r}}\right]^{1/2}, \tag{27}$$

where

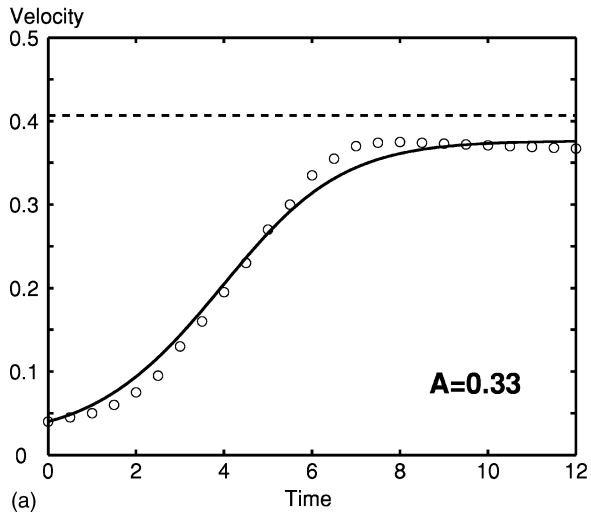

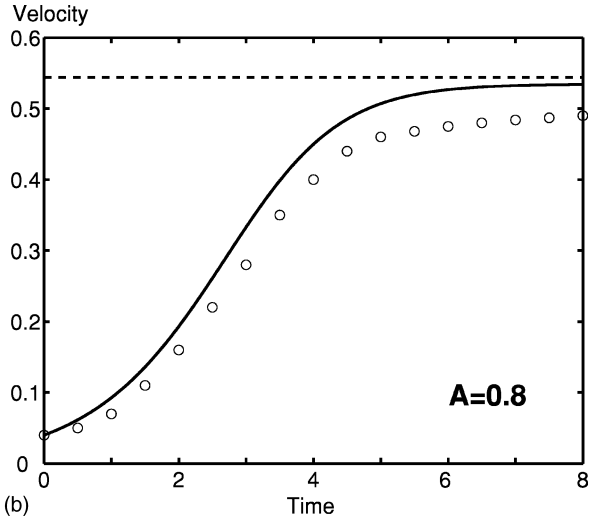

FIG. 3. Comparisons for bubble velocities in the RT instability in 2D. Atwood numbers are (a) $A=0.33$, (b) $A=0.8$. Solid curves are predictions from the present model, dashed lines are the asymptotic solution (23) from Ref. [13], and symbols are numerical results taken from Ref. [15]. The x and y axes correspond to dimensionless time and dimensionless velocity, scaled as $t\sqrt{gk}$ and $\nu\sqrt{k/g}$, respectively.

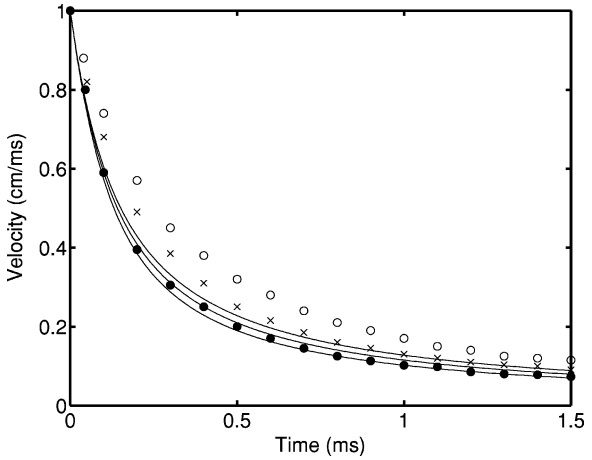

FIG. 4. Comparisons for bubble velocities in the RM instability in 2D. The solid curves are predictions from the present model for $A=0.2$, 0.5, and 0.9 from above to below. Symbols are numerical results taken from Ref. [8]: ○, $A=0.2$; ×, $A=0.5$; ●, $A=0.9$.

$$G(h)=\frac{1}{(2k)^{2r}}\left\{\ln\left(\frac{(Q^r+(2k)^r)^2}{Q^{2r}-(2k)^rQ^r+(2k)^{2r}}\right)+2\sqrt{3}\tan^{-1}\left(\frac{4^rQ^r-k^r}{\sqrt{3}k^r}\right)\right\}+\frac{1}{Q^{2r}},$$

$$Q(h)=(6\xi_0+k)e^{-3k(h-h_0)}.$$

Here, $G_0=G(h_0)$, $Q_0=Q(h_0)$, and $r=\frac{1}{3}$. From Eq. (27), the height of bubble tip at time t is implicitly given by

$$t(h)=\int_{h_0}^{h}\frac{(2k)^{1/2}Q_0^r}{Q(\tau)^r[AgQ_0^{2r}(G(\tau)-G_0)+2k\nu_0^2]^{1/2}}d\tau. \tag{28}$$

Thus, we obtained analytic solutions for ν and ξ over all times for $A\to 0$. Giving the bubble height h, time t is determined by Eq. (28), ξ by Eq. (15), and ν by Eq. (27). Note that the analytic expression for finite time solutions for the case of $A=1$ is given in Refs. [9,10].

The present model is validated by comparing with results of numerical simulations in two dimensions. In Fig. 3, we compare the solutions from the present model for a bubble of the Rayleigh-Taylor instability with numerical results from the vortex method in Ref. [15] and the asymptotic solution (23) from Ref. [13]. The vortex simulations in [15] are performed in incompressible fluids, following the marker particles on the interface in Lagrangian manner. The Atwood numbers for Fig. 3(a) and Fig. 3(b) are $A=0.33$ and $A=0.8$, respectively. For both cases, g and k are set to 1 and initial conditions are $\nu_0=0.04$, $h_0=0.049$, and $\xi_0=-0.022$. We see that the predictions from the present model are in good agreement with the numerical results.

Figure 4 shows the comparison of the solutions from the present model for a Richtmyer-Meshkov bubble with numerical results in Ref. [8] for three cases of Atwood numbers $A=0.2$, 0.5, and 0.9. The results in Ref. [8] are obtained from full-scale simulations of two-dimensional Euler equations in incompressible limit. Physical parameters are set to $g=0$ and $k=2\pi$ cm^{-1} and initial conditions are $\nu_0=1$ cm/ms, $h_0=0$, and $\xi_0=0$. We observe that asymptotic decaying rates agree well for all three cases and, at early times, the results for larger values of A are in better agreement.

The results for bubbles in two dimensions can be directly extended to bubbles in three-dimensional cylindrical geometry. The bubble motion in 3D was first studied by Layzer [14] for the system of infinite density ratio. Extending again Layzer's, we take the potentials

$$\phi(r,z,t)=a(t)J_0(\beta_1 r/R)e^{-\beta_1 z/R}, \tag{29}$$

$$\phi'(x,z,t)=-a(t)J_0(\beta_1 r/R)e^{-\beta_1 z/R}, \tag{30}$$

where R is the radius of a cylindrical channel and β_1 is the first zero of the Bessel function $J_1(r)$. Then, differential equations for dynamics of bubbles in 3D are

$$\frac{dh}{dt}=-ake^{-kh}, \tag{31}$$

$$\frac{d\xi}{dt}=ak^2\left(2\xi+\frac{k}{4}\right)e^{-kh}, \tag{32}$$

$$ke^{-kh}\left(\xi+\frac{k}{4}\right)\frac{da}{dt}+Aa^2k^3\left(\xi+\frac{k}{8}\right)e^{-2kh}=Ag\xi, \tag{33}$$

where $k=\beta_1/R$. Applying the same procedures as in 2D, we give the asymptotic solutions for RT and RM bubbles in 3D:

$$\nu_{\mathrm{RT}}^{\infty}\to\sqrt{\frac{AgR}{\beta_1}},\quad \xi_{\mathrm{RT}}^{\infty}\to-\frac{\beta_1}{8R}, \tag{34}$$

and

$$\nu_{\mathrm{RM}}^{\infty}\sim\frac{R}{\beta_1 t},\quad \xi_{\mathrm{RM}}^{\infty}\to-\frac{\beta_1}{8R}. \tag{35}$$

The validation study for these solutions in 3D is being carried out. This result will be published elsewhere.

In conclusion, the Layzer-type model has been extended to the unstable system for all A, using simple forms of velocity potentials. I have shown, through comparisons with numerical results, that the present model provides a comprehensive theory for the evolution of RT and RM bubbles over all time ranges from the small amplitude linear stage to the late nonlinear stage.

This work was supported by Grant No. R01-2000-00002 from the Basic Research Program of the Korea Science & Engineering Foundation.

[1] Lord Rayleigh, *Scientific Papers* (Cambridge University Press, Cambridge, England, 1900), Vol. II, p. 200.
[2] R.D. Richtmyer, Commun. Pure Appl. Math. **13**, 297 (1960).
[3] J. Glimm and D.H. Sharp, Phys. Rev. Lett. **64**, 2137 (1990); J. Glimm, D. Saltz, and D.H. Sharp, *ibid.* **80**, 712 (1998).
[4] N.J. Zabusky, Annu. Rev. Fluid Mech. **31**, 495 (1999).
[5] J.W. Jacobs and I. Catton, J. Fluid Mech. **187**, 329 (1988).
[6] M.J. Dunning and S.W. Hann, Phys. Plasmas **2**, 1669 (1995).
[7] J. Hecht, U. Alon, and D. Shvarts, Phys. Fluids **6**, 4019 (1994).
[8] U. Alon, J. Hecht, D. Ofer, and D. Shvarts, Phys. Rev. Lett. **74**, 534 (1995).
[9] Q. Zhang, Phys. Rev. Lett. **81**, 3391 (1998).
[10] K.O. Mikaelian, Phys. Rev. Lett. **80**, 508 (1998).
[11] S.-I. Sohn and Q. Zhang, Phys. Fluids **13**, 3493 (2001).
[12] S.I. Abarzhi, Phys. Rev. Lett. **81**, 337 (1998).
[13] V.N. Goncharov, Phys. Rev. Lett. **88**, 134502 (2002).
[14] D. Layzer, Astrophys. J. **122**, 1 (1955).
[15] R.M. Kerr, J. Comput. Phys. **76**, 48 (1988).